

# Influence of Substrate Stiffness on the Phenotype of Heart Cells

Bashir Bhana,<sup>1</sup> Rohin K. Iyer,<sup>2</sup> Wen Li Kelly Chen,<sup>2</sup> Ruogang Zhao,<sup>2</sup> Krista L. Sider,<sup>2</sup> Morakot Likhitanichkul,<sup>3</sup> Craig A. Simmons,<sup>2,3,4</sup> Milica Radisic<sup>1,2</sup>

<sup>1</sup>Department of Chemical Engineering and Applied Chemistry, University of Toronto, 164 College St, Rm. 407, Toronto, Ontario, Canada; telephone: 416-946-5295; fax: 416-978-4317; e-mail: m.radisic@utoronto.ca

<sup>2</sup>Institute of Biomaterials and Biomedical Engineering, University of Toronto, Toronto, Ontario, Canada

<sup>3</sup>Department of Mechanical and Industrial Engineering, University of Toronto, Toronto, Ontario, Canada

<sup>4</sup>Faculty of Dentistry, University of Toronto, Toronto, Ontario, Canada

Received 21 August 2009; revision received 30 November 2009; accepted 4 December 2009

Published online 15 December 2009 in Wiley InterScience (www.interscience.wiley.com). DOI 10.1002/bit.22647

**ABSTRACT:** Adult cardiomyocytes (CM) retain little capacity to regenerate, which motivates efforts to engineer heart tissues that can emulate the functional and mechanical properties of native myocardium. Although the effects of matrix stiffness on individual CM have been explored, less attention was devoted to studies at the monolayer and the tissue level. The purpose of this study was to characterize the influence of substrate mechanical stiffness on the heart cell phenotype and functional properties. Neonatal rat heart cells were seeded onto collagen-coated polyacrylamide (PA) substrates with Young's moduli of 3, 22, 50, and 144 kPa. Collagen-coated glass coverslips without PA represented surfaces with effectively "infinite" stiffness. The local elastic modulus of native neonatal rat heart tissue was measured to range from 4.0 to 11.4 kPa (mean value of 6.8 kPa) and for native adult rat heart tissue from 11.9 to 46.2 kPa (mean value of 25.6 kPa), motivating our choice of the above PA gel stiffness. Overall, by 120 h of cultivation, the lowest stiffness PA substrates (3 kPa) exhibited the lowest excitation threshold (ET;  $3.5 \pm 0.3$  V/cm), increased troponin I staining (52% positively stained area) but reduced cell density, force of contraction ( $0.18 \pm 0.1$  mN/mm<sup>2</sup>), and cell elongation (aspect ratio = 1.3–1.4). Higher stiffness (144 kPa) PA substrates exhibited reduced troponin I staining (30% positively stained area), increased fibroblast density (70% positively stained area), and poor electrical excitability. Intermediate stiffness PA substrates of stiffness

comparable to the native adult rat myocardium (22–50 kPa) were found to be optimal for heart cell morphology and function, with superior elongation (aspect ratio > 4.3), reasonable ET (ranging from  $3.95 \pm 0.8$  to  $4.4 \pm 0.7$  V/cm), high contractile force development (ranging from  $0.52 \pm 0.2$  to  $1.60 \pm 0.6$  mN/mm<sup>2</sup>), and well-developed striations, all consistent with a differentiated phenotype.

Biotechnol. Bioeng. 2010;xxx: xxx–xxx.

© 2009 Wiley Periodicals, Inc.

**KEYWORDS:** substrate stiffness; cardiomyocyte; fibroblast; heart; hydrogel; contraction

## Introduction

Myocardial infarction caused by ischemia is one of the leading causes of mortality in the world. Adult heart tissue retains little capacity for regeneration, which motivates studies in cardiac tissue engineering. Though contractile cardiomyocytes (CM) represent only approximately one-third of the cells in the adult myocardium, they occupy 80–90% of its volume and have no significant ability to proliferate (Nag, 1980). The remaining two-third of cells are non-myocytes such as endothelial cells (EC) and fibroblasts (FB) which have a capacity to proliferate. Understanding how a cell's extracellular environment, and in particular matrix stiffness, influences cell morphology and function has important implications for the design of biomaterials for cardiac tissue engineering. While influence of matrix stiffness on individual CM has been well studied (Engler et al., 2008; Jacot et al., 2008), less attention was devoted to

Bashir Bhana and Rohin K. Iyer contributed equally to this work.

Correspondence to: M. Radisic

Contract grant sponsor: Heart and Stroke Foundation of Ontario (HSFO)

Contract grant number: NA 6077; NA6047

Contract grant sponsor: National Sciences and Engineering Research Council of Canada Discovery Grants

Contract grant number: RGPIN 326982-06; RGPIN 327627-06

Contract grant sponsor: Ontario Early Researcher Award

Contract grant sponsor: Canada Research Chair in Mechanobiology

Additional Supporting Information may be found in the online version of this article.

the effects of the matrix stiffness at the monolayer and tissue levels. Only few studies examined the influence of matrix stiffness on the structure and function of engineered heart tissues (EHTs; Engelmayer et al., 2008; Shapira-Schweitzer and Seliktar, 2007). An ideal engineered tissue should consist of multiple cell types (e.g., CM and FBs) as in the native heart. Thus, elucidating the effects of the matrix stiffness on the relative cell fractions in this heterogeneous population is required.

Hydrogel substrates are commonly used to test the influence of matrix stiffness on cell function (Drury and Mooney, 2003; Pelham and Wang, 1997; Peyton et al., 2006). Synthetic polymers (e.g., polyacrylamide, PA) provide control of the cell microenvironment and do not interfere with microscopy as they are optically clear. Since they are cell-repellent, they are modified with ligands whose density can be varied independently of mechanical properties. Their elastic modulus can be tuned by varying the cross-linker concentration. PA gels, which consist of acrylamide monomers cross-linked by bis-acrylamide, were first used to demonstrate the effect of substrate stiffness on epithelial cells and FB (Pelham and Wang, 1997).

The main objective of this study was to characterize the influence of substrate stiffness on the morphology and contractile properties of cell monolayers isolated from neonatal rat hearts. The cells were seeded on collagen I coated PA gels of stiffness varying from 3 to 144 kPa. Collagen was chosen because it is highly expressed in the extracellular matrix of native cardiac muscle tissue. We evaluated a heterogeneous population consisting of both CM and FB, since these mixed populations were found to be beneficial for cardiac tissue engineering (Caspì et al., 2007; Chiu et al., 2008; Iyer et al., 2008, 2009; Levenberg et al., 2005; Naito et al., 2006; Radisic et al., 2008a,b). We hypothesized that substrate stiffness comparable to that of the native myocardium would be conducive to the differentiated phenotype of neonatal rat CM. Knowledge of the substrate stiffness that supports differentiated phenotype of heart cells may be useful in the rational design of scaffolds and hydrogels for cardiac tissue engineering.

## Materials and Methods

### Neonatal Rat CM Isolation

Primary CMs were harvested from neonatal rats according to a protocol approved by the University of Toronto

Committee on Animal Care. The cells were isolated by serial collagenase digestion and enriched slightly for CM by one cycle of pre-plating as previously described (Chiu et al., 2008; Iyer et al., 2008, 2009; Radisic et al., 2008a).

### PA Substrate Fabrication, Collagen Functionalization, and Characterization

The PA substrates were fabricated (Chen et al., in press) between two glass slides using a protocol adapted from Pelham and Wang (1997). Briefly, PA substrates of increasing stiffness were obtained by varying the concentration of acrylamide (3.0–15%; BioRad, Mississauga, ON) and bis-acrylamide (0.10–1.2%) in de-ionized water and 10 mM HEPES (Sigma, Oakville, ON; Table I) as described in detail in the Supplemental Information. Upon photopolymerization, the gels were incubated in 7 µg/mL rat tail type I collagen solution (BD, Mississauga, ON) at 4°C overnight followed by rinsing in phosphate buffered saline (PBS) and UV sterilization for 20 min. We have shown elsewhere that the collagen coating concentration is independent of PA gel stiffness (Chen et al., in press). Control glass cover slips were similarly coated with collagen.

To determine elastic moduli and Poisson's ratios, fully hydrated cylindrical PA specimens were subjected to 10% static unconfined compressive strain with a ramp velocity of 1 µm/s, and held to allow for stress relaxation until equilibrium was reached (Chen, in press). The Young's moduli of the PA gels were calculated from the ratio of the recorded stress at equilibrium and the applied strain. The Poisson's ratios were calculated as axial to radial strain, with the radial strain determined by imaging lateral expansion of the gels at equilibrium.

The gels were dehydrated in serial grades of ethanol (50%, 70%, and 100%), critical point dried, sputter coated with gold and imaged using a Hitachi S-570 Scanning Electron Microscope (SEM) as described by Iyer et al. (2008). To reveal the PA pores, the gels were fractured, sputter coated with gold, and imaged in the cross-section.

### Cell Seeding

Prior to cell seeding, the PA gels were primed with 1 mL of cardiac culture medium for 24 h at 37°C (5% CO<sub>2</sub>) to remove residual cross-linker. The culture medium was removed and each hydrogel was seeded with 15 µL of cell suspension (containing  $1 \times 10^5$  cells). The cells were

**Table I.** Mechanical properties of PA hydrogels.

Composition (%acrylamide/%bis-acrylamide)	Young's modulus (kPa; Chen et al., in press)	Poisson's ratio
3%/0.1%	3.4 ± 0.5	0.33 ± 0.06
8%/0.2%	22.5 ± 9.5	0.30 ± 0.10
15%/0.3%	50.3 ± 4.6	0.37 ± 0.06
15%/1.2%	144.5 ± 6.6	0.44 ± 0.04

incubated at 37°C (5% CO<sub>2</sub>) for 30 min in 12-well plates, followed by the addition of 1 mL of culture medium. The cells were cultivated for 120 h and their medium replaced every 36 h. Cardiac medium was 88% high glucose Dulbecco's modified Eagle's medium (DMEM), 10% fetal bovine serum (FBS), 1% (1 M) 4-(2-hydroxyethyl)-1-piperazineethanesulfonic acid (HEPES) buffer, and 1% penicillin–streptomycin (100 U/mL).

### Functional Testing

The excitation threshold (ET, minimum electric field strength for synchronous excitation at 1 Hz) and maximum capture rate (MCR, maximum sustained synchronous beating rate, measured at 2× the ET) were measured at 120 h in response to electrical field stimulation as previously described (Chiu et al., 2008; Iyer et al., 2008, 2009; Radisic et al., 2004; Tandon et al., 2009) using 2 ms square monophasic pulses and voltage up to 10 V/cm, above which constructs were deemed to be non-contracting.

### Contraction Force

CM contraction was characterized by measuring the displacement of fluorescent beads physically embedded in the gel by video fluorescence microscopy (Olympus Canada, Markham, ON, Model IX81) at 120 h as described in detail in Supplemental Information ( $n \geq 3$ ). Videos were obtained using QED Imaging<sup>TM</sup> In Vitro Software, version 3.1.0 (Media Cybernetics Inc., Bethesda, MD). Samples were stimulated with square, monophasic 2 ms pulses at an electric field strength of 12 V/cm. This was sufficiently higher than the ET of all samples to ensure synchronous contractions in even the least contractile cells. To approximate the relative stresses generated in the substrates by CM contraction, the measured displacement fields were used to prescribe displacements in a two-dimensional (2D) plane stress finite element model representing the hydrogel (Yang et al., 2006). The hydrogels were modeled as isotropic and linear elastic with moduli and Poisson's ratios determined experimentally (Table I). The shear modulus,  $G$ , for an isotropic elastic material is dependent on the Young's modulus,  $E$ , and Poisson's ratio ( $G = E/2(1 + \nu)$ ), and therefore only two of these three parameters are necessary to fully define the elastic behavior of the material. The model was analyzed using ANSYS (Canonsburg, PA) to estimate the resulting strain and stress distributions for several cells per image. To eliminate modeling artifacts, only mid-95th percentile stress and strain values were used to characterize CM contraction.

### Tissue Mechanical Testing

One neonatal (1- to 2-day old) and one adult Sprague–Dawley rat heart were kept at 4°C in Hank's Balanced Salt Solution (HBSS) without Mg<sup>2+</sup> or Ca<sup>2+</sup> until mechanical testing could be performed (~1-h postmortem). Local tissue

mechanical properties were determined by micropipette aspiration (MA) of the distal wall and left ventricle wall (Aoki et al., 1997). The hearts were maintained mostly submerged in PBS with Ca<sup>2+</sup> and Mg<sup>2+</sup>. The area just around the test site was exposed to air during the test (~10 min) to aid visualization and re-hydrated between tests. PBS-filled pipettes of 1.038 mm ID (adult) and 0.58 mm ID (neonatal) were used to apply pressure locally. These diameters maintained a tissue thickness to pipette diameter ratio >1 to ensure the mechanical properties of the wall tissue were measured. Pipette placement was controlled by a micromanipulator. Pressure was applied using a 5 mL syringe attached to a linear actuator, which applied ~5 kPa steps to a maximum applied pressure of 30–35 kPa. Images were captured immediately after each step using a stereoscope (Olympus S761, Markham, ON) connected to a digital camera (Canon, Mississauga, ON), from which aspiration lengths were measured at each pressure level. Five spots on each heart were tested. No drying of the hearts was observed during testing. The initial elastic modulus (representative of the physiological range; Engelmayer et al., 2008) was estimated using an analytical half-space model that is commonly applied to analyze MA data (Theret et al., 1988; see Supplemental Fig. 1).

### Cell Phenotype and Viability

For viability and cell density evaluation at 120 h, live cells were stained with carboxyfluorescein diacetate succinimidyl ester (CFDA) and dead cells with propidium iodide (PI; Iyer et al., 2008). Briefly, a solution of 10 μM CFDA and 2.5 μg/mL PI in PBS was applied to the cells for 40 min at 37°C. For immunostaining, cells were fixed in 4% paraformaldehyde (PFA) for 1 h at room temperature and stained for cardiac troponin I to identify CM and vimentin to identify non-myocytes, according to protocols we have described (Brown et al., 2008; Iyer et al., 2008; Radisic et al., 2008a). Primary antibodies were polyclonal rabbit anti-cardiac troponin I (Chemicon, Etobicoke, ON, 1:150) and Cy3-conjugated mouse monoclonal anti-vimentin (Sigma, 1:50). Isotype controls were rabbit IgG and mouse IgG1. The analysis of cell length and aspect ratio (length/width) was performed from immunostained images after 12 and 120 h as described by Au et al. (2007), Radisic et al. (2008a), and Tandon et al. (2009).

### Statistical Analysis

Analyses were performed using one-way ANOVA and SigmaStat software (SPSS, Chicago, IL) with  $P < 0.05$  considered to be statistically significant.

## RESULTS

### Characterization of Native Heart and PA Hydrogels

The local elastic moduli of the neonatal rat heart tissue ranged from 4.0 to 11.4 kPa ( $6.8 \pm 2.8$  kPa). Local moduli

for adult rat heart tissue ranged from 11.9 to 46.2 kPa ( $25.6 \pm 15.9$  kPa; Supplemental Fig. 1). These results motivated our choice of the PA gel moduli, which ranged from 3 to 144 kPa (Chen et al., in press; Table I). The Poisson's ratio range we measured for PA gels was similar to that used by others (e.g.,  $\nu = 0.4$ , Yang et al., 2006; Table I). SEM indicated that the top surface of all hydrogels was smooth, regardless of the stiffness, resulting from the hydrogel fabrication between two coverslips (Fig. 1A). All hydrogels were coated with scattered collagen globules of approximately equal density (Fig. 1A). The cross-sectional images (Fig. 1B) indicated the presence of porous structure in the gel interior, that was not directly accessible to the cells seeded on the top smooth surface.

### Contractile Properties of Heart Cells on PA Hydrogel Substrates

Spontaneous contractions were observed on the 5th day of cultivation on the 3, 22, and 50 kPa substrates. Sustained spontaneous contraction was predominant on the 22 and 50 kPa substrates. Minimal to no spontaneous contraction was observed on the 144 kPa and glass substrates. The ETs showed an increasing trend with increasing stiffness, ranging from  $3.5 \pm 0.3$  V/cm for the 3 kPa constructs to  $4.4 \pm 0.7$  V/cm for the 50 kPa constructs (Fig. 2). Cells on the 50 kPa PA hydrogel displayed an ET that was significantly higher than that of the 3 kPa stiffness, but neither was significantly different from the 22 kPa stiffness. The average MCR was not significantly different between the three groups that exhibited synchronous contractions. Cells on 144 kPa stiffness PA hydrogels and glass substrates could not be induced to beat synchronously with application of an electric field of up to 10 V/cm, although beating of some individual cells was observed. As a result, no functional data could be obtained for these groups.

For contraction force measurements, the cells were stimulated at 12 V/cm, ensuring that beating was observed in all groups including the 144 kPa group, for which isolated cell clusters were beating (Fig. 3). Glass control substrates were excluded from the analysis as no fluorescent beads could be embedded. The mean displacement of the fluorescent microspheres decreased with increasing stiffness of the gels (Fig. 3A). The strain, accordingly, also decreased with increasing stiffness (Fig. 3B), with the 3 kPa stiffness gels displaying a larger strain than the 22 and 144 kPa groups ( $P < 0.05$ ). The contraction force per unit area exerted by the cells (Fig. 3C) increased with increasing gel stiffness and was significantly different amongst the groups ( $P < 0.05$ ) except 3 kPa versus 22 kPa, which exhibited no significant difference.

### Cell Viability and Density

No marked differences in cell viability were observed with an increase in the PA gel stiffness (Supplemental Fig. 2). For the

3 and 144 kPa substrates, the viability increased from  $\sim 60\%$  at 12 h to just over 80% at 120 h of cultivation (Fig. 4A). The viability of cells seeded on glass alone decreased significantly from  $\sim 80\%$  at 12 h to below 60% at 120 h (Fig. 4A). At 12-h incubation, total cell density remained unchanged with increasing stiffness. At 120 h, total cell density significantly increased with increasing stiffness in all groups except the 3 kPa PA surfaces (Fig. 4B).

### Immunostaining for Cell-Specific Markers

Since this work was intended at determining the hydrogel stiffness most suitable for cardiac tissue engineering, the heart cell isolate after one pre-plating step was used in all experiments to ensure that effects of stiffness on both myocytes and non-myocytes were being considered. The cells appeared mostly spherical 12 h after seeding and they elongated at 120 h (Supplemental Fig. 3). In order to distinguish between CM and FB, double staining for troponin I, a contractile protein of CM, and vimentin, an intermediate filament of non-myocytes, was performed (Fig. 5) with isotype controls confirming primary antibody specificity (Supplemental Fig. 4). At the early time point, 12 h, a higher number of cells is observed in Supplemental Figure 3 compared to Figure 5. The large number of round cells in Supplemental Figure 3, may simply be settled rather than truly attached cells. An aspect ratio (the ratio of cell axial length to radial width) of  $\sim 1$  is expected for spherical cells, as observed for all groups at 12 h (Fig. 6), while an aspect ratio greater than 1 is expected for elongated cells. After 120 h of cultivation, significant levels of FB elongation were observed for 22, 50, and 144 kPa substrates (Fig. 6A and C), while significant CM elongation was observed for 50 and 144 kPa substrates (Fig. 6B and D). Overall, the 50 kPa substrate had the highest average length and aspect ratio in all groups. Cells on the 3 kPa and glass substrates exhibited minimal elongation after 120 h. Interestingly, at every time point, for every group there were no significant differences in the aspect ratio between FB and CM. The same was true for the cell length measurements except for the glass substrate after 120 h, where FB were longer than CM and 22 kPa substrate at 12 h, where CM were longer than FB. Thus, average area covered by each cell type was used to determine the relative presence of each cell type on the surface.

At 12-h incubation, the percentage of area stained for troponin I, increased with increasing PA stiffness, while opposite trend was observed for vimentin staining (Fig. 7). At 120-h incubation, the troponin I stained area showed a decreasing trend with increasing PA stiffness (Fig. 7A), while vimentin increased (Fig. 7B). A greater number of cells exhibiting developed striations were present in the 22 kPa (Fig. 8ii) and 50 kPa (Fig. 8iii) groups, compared to the 3 kPa (Fig. 8i), 144 kPa (Fig. 8iv) and glass (Fig. 8v) groups. Although spread, CM were circular instead of rod-shaped on the glass substrates (Fig. 8), consistent with the aspect ratio

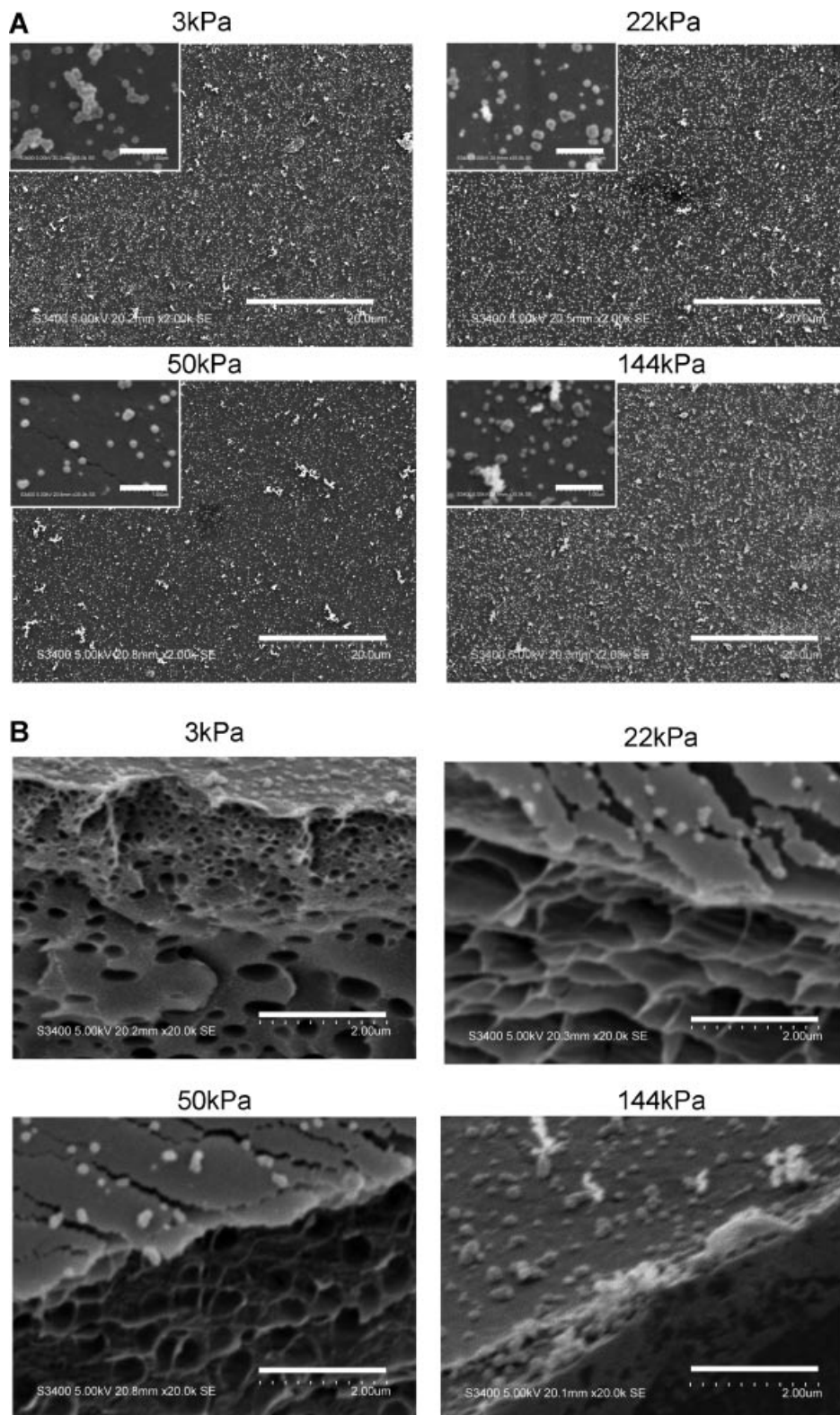


**Figure 1.** Scanning electron micrographs of PA hydrogels. **A:** The top view indicates smooth surfaces with scattered collagen droplets of approximately equal density. Scale bar: 20  $\mu\text{m}$ . Inset: 1  $\mu\text{m}$ . **B:** Cross-sectional view indicates the presence of the pores in the hydrogel interior. Scale bar: 2  $\mu\text{m}$ .

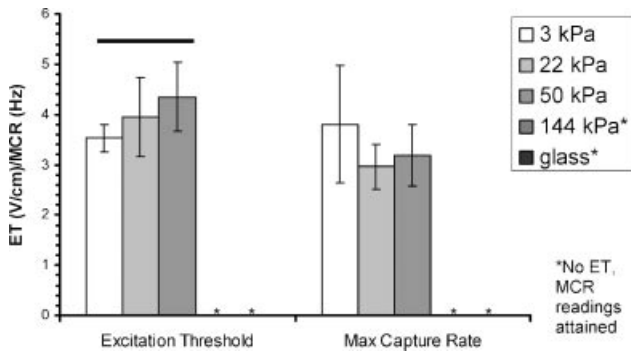


**Figure 2.** Construct contractile properties as a function of substrate stiffness. **A:** The excitation threshold (ET) and maximum capture rate (MCR). The symbol (\*) denotes groups for which ET and MCR could not be measured due to cells not responding to a stimulus of up to 10V/cm. Horizontal bars denote statistically significant differences at a  $P < 0.05$  using one-way ANOVA.

measurement of  $\sim 1.7$ . On hydrogel substrates, rod-shaped CM were observed (Fig. 8). In Figure 8, cells of which only the nuclei stain could be smooth muscle cells, present in the native heart cell isolates at 3–4% after one pre-plating step (Brown et al., 2008; Naito et al., 2006).

## Discussion

The main purpose of this study was to determine the role of substrate stiffness on the morphology and functional properties of heart cells. The cells were slightly enriched for CM by one pre-plating step and seeded at high density, conditions commonly used in cardiac tissue engineering (Radisic et al., 2003). Previous studies (Naito et al., 2006; Radisic et al., 2008b) demonstrated that the population consisting of FB and CM resulted in improved morphological and functional properties of the EHT in comparison to the cells significantly enriched for CM.

Significant efforts have been made to improve the morphological and functional properties of CM in monolayers and EHT through the design of substrates with topographical cues (Au et al., 2007; Bursac et al., 2002) and design of bioreactors for mechanical (Zimmermann et al., 2002) or electrical stimulation (Radisic et al., 2004). However, the effect of substrate stiffness remains largely unstudied. Recently, Jacot et al. (2008) demonstrated that substrate stiffness affected the functional maturation of neonatal rat ventricular CM and that optimal sarcomere structure was obtained for cells on 10 kPa substrates. Neonatal rat CM cultured in three-dimensional (3D) PEGylated fibrinogen gels were demonstrated to aggregate and beat, forming a larger region of contraction on compliant gels (8 Pa shear modulus) as compared to more rigid gels (341 Pa shear modulus; Shapira-Schweitzer and Seliktar, 2007).

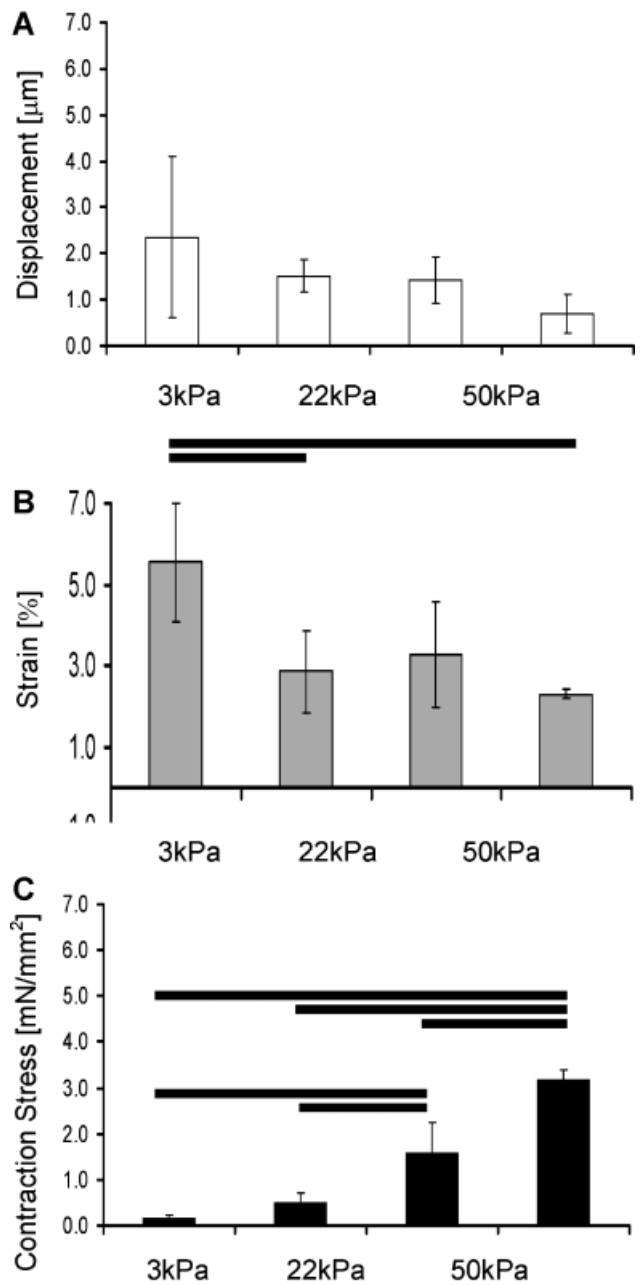


**Figure 3.** Contraction stress measurements of heart cells cultivated on PA hydrogels. **A:** Mean displacement, **(B)** mean strain, and **(C)** contraction stress exerted by cells on the PA gels were calculated by measuring the movement of fluorescent microspheres embedded throughout the PA gels. Error bars denote standard deviation. Statistical analysis performed using one-way ANOVA,  $P < 0.05$  considered statistically significant,  $n = 9$ . Due to the non-deformable nature of glass ( $\sim$ infinite stiffness), readings are not shown for this group.

The effect of substrate stiffness on proliferation and phenotype of non-myocytes (EC, FB, neutrophils, hepatocytes, chondrocytes) has been more extensively studied (Pelham and Wang, 1997; Semler et al., 2000; Subramanian and Lin, 2005; Yeung et al., 2005). EC and FB exhibited reduced spreading, increased migration, and elevated

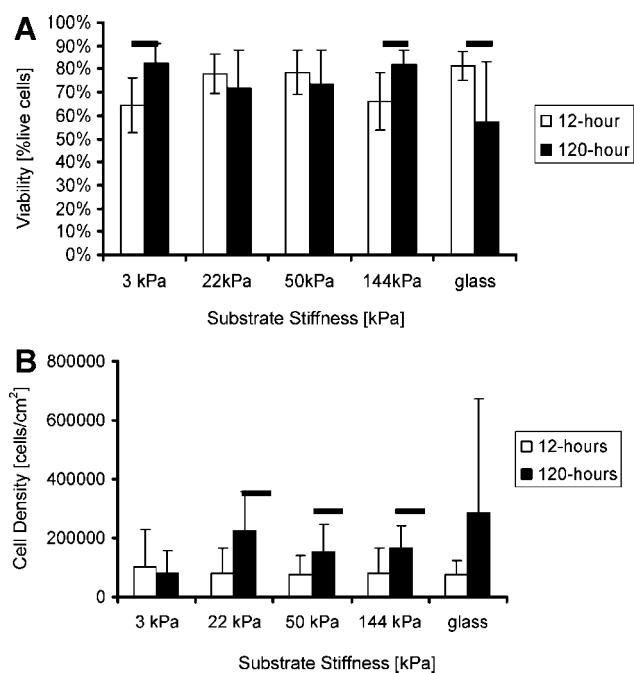


**Figure 4.** Cell viability and density at 12 and 120 h of cultivation. **A:** Cell viability expressed as a percentage of live cells relative to the total cell count. **B:** Cell density. Error bars denote standard deviation. Statistical analysis performed using one-way ANOVA,  $P < 0.05$  considered statistically different. The viability and density was determined from two independent experiments. There were between three and four samples per group, with three pictures per sample taken at 10 $\times$ . All cells were counted in each picture. On average, 1,800 cells were counted per group at 12 h and 4,100 cells per group at the 120 h time point.

lamellipodial protrusions on less stiff substrates (Lo et al., 2000; Pelham and Wang, 1997). On rigid substrates, they formed stable focal adhesions and generated greater traction forces (Lo et al., 2000; Pelham and Wang, 1997). The present study characterizes the influence of substrate stiffness on the development of differentiated phenotype and contractile properties of heart cells cultivated on substrates with elastic moduli of 3, 22, 50, 144 kPa and glass as a nearly infinite stiffness substrate. All substrates were coated with the same non-limiting amount of collagen I to ensure that the presence of adhesive cues was identical amongst the groups (Fig. 1). Thus, any observed changes in cell phenotype were due to substrate stiffness. This approach has been used by others (Jacot et al., 2008) to decouple the effects of ligand density and substrate stiffness. The gels in this experiment were  $\sim 180 \mu\text{m}$  thick. For gels prepared using the same procedure, Engler et al. have shown thickness independence down to  $5 \mu\text{m}$ , below which the traction forces generated by the cells were influenced by the rigid glass beneath the gel (Engler et al., 2004b).

In committed cells, regulation of differentiation is dependent on the substrate stiffness, as demonstrated with skeletal muscle cells (Engler et al., 2004a). Cells exhibit their differentiated phenotype on substrates that match the stiffness of their native ECM (Engler et al., 2004a, 2006).

Thus, we hypothesized that differentiated phenotype of heart cells as measured by cell elongation, contraction, and presence of cell-specific markers will be the most prominent on substrates with stiffness comparable to that of the native heart. The stiffness of the neonatal (4.0–11.4 kPa) and adult rat myocardium (11.9–46.2 kPa) measured here were in a reasonable agreement with previously reported values. The stiffness of the adult rat myocardium was reported to be  $\sim 70 \text{ kPa}$  (Boublik et al., 2005), while the stiffness of the adult rat right ventricle was reported to be  $54 \pm 8 \text{ kPa}$  in the circumferential direction and  $20 \pm 4 \text{ kPa}$  in the longitudinal direction (Engelmayr et al., 2008). Adult rat left ventricle was measured to have the stiffness of  $18 \pm 2 \text{ kPa}$  by atomic force microscopy (Berry et al., 2006).

We demonstrated that 3D cardiac constructs had an ET of 2.5 V and MCR of 5.8 Hz (Radisic et al., 2004). A lower ET and higher MCR are indicative of more complete electrical and cellular connections between CM (Radisic et al., 2004). The higher ET and lower MCR in this study (Fig. 2) compared to cardiac constructs may in part be explained by the 2D nature of the monolayers in the present study, with fewer cell–cell connections in 2D compared to 3D constructs. Force of contraction is influenced by the extent to which cell–cell contacts are formed but substrate rigidity may override this (Yeung et al., 2005). The displacement of the fluorescent beads during CM contraction, stimulated by identical voltages of 12 V/cm for all groups, decreased with increasing gel stiffness (Fig. 3A). Conversely, the force of contraction per unit area was directly proportional to the PA gel stiffness (Fig. 3C), increasing with increasing gel stiffness. This suggests that the force generation by CM can be predictably influenced by the substratum on which they are seeded. The reported displacement (Fig. 3A) includes both the displacement of the beads relative to the PA gel and the rigid body movement of the PA gel through the field of view. The strains were calculated based on differences between bead displacements, which eliminate rigid body movement. Thus, although there may be no significant difference in total displacements, there can be significant differences in the calculated strains (Fig. 3B) and stresses (Fig. 3C), as was the case here. The contraction stress is related to the stiffness of the gel through the strain. Thus, the contraction force trend over multiple gel types depends not only on the individual gel stiffness but also the trend with which strains change on different gels. It is possible that contraction force may not increase proportionally with gel stiffness, depending on the relative strain response. However, in this case we did observe that contraction force (Fig. 3C) was proportional to gel stiffness (Fig. 3B).

In order to determine the substrate stiffness that yields desirable functional properties in heart cells, electrical excitability (Fig. 2), and contraction force data (Fig. 3) need to be considered simultaneously. The cells on the 144 kPa PA gels and the infinite stiffness glass substrates could be not induced to contract synchronously using reasonable voltages up to 10 V/cm (Fig. 2). Thus, for the contraction force measurement, the stimulation voltage was increased to

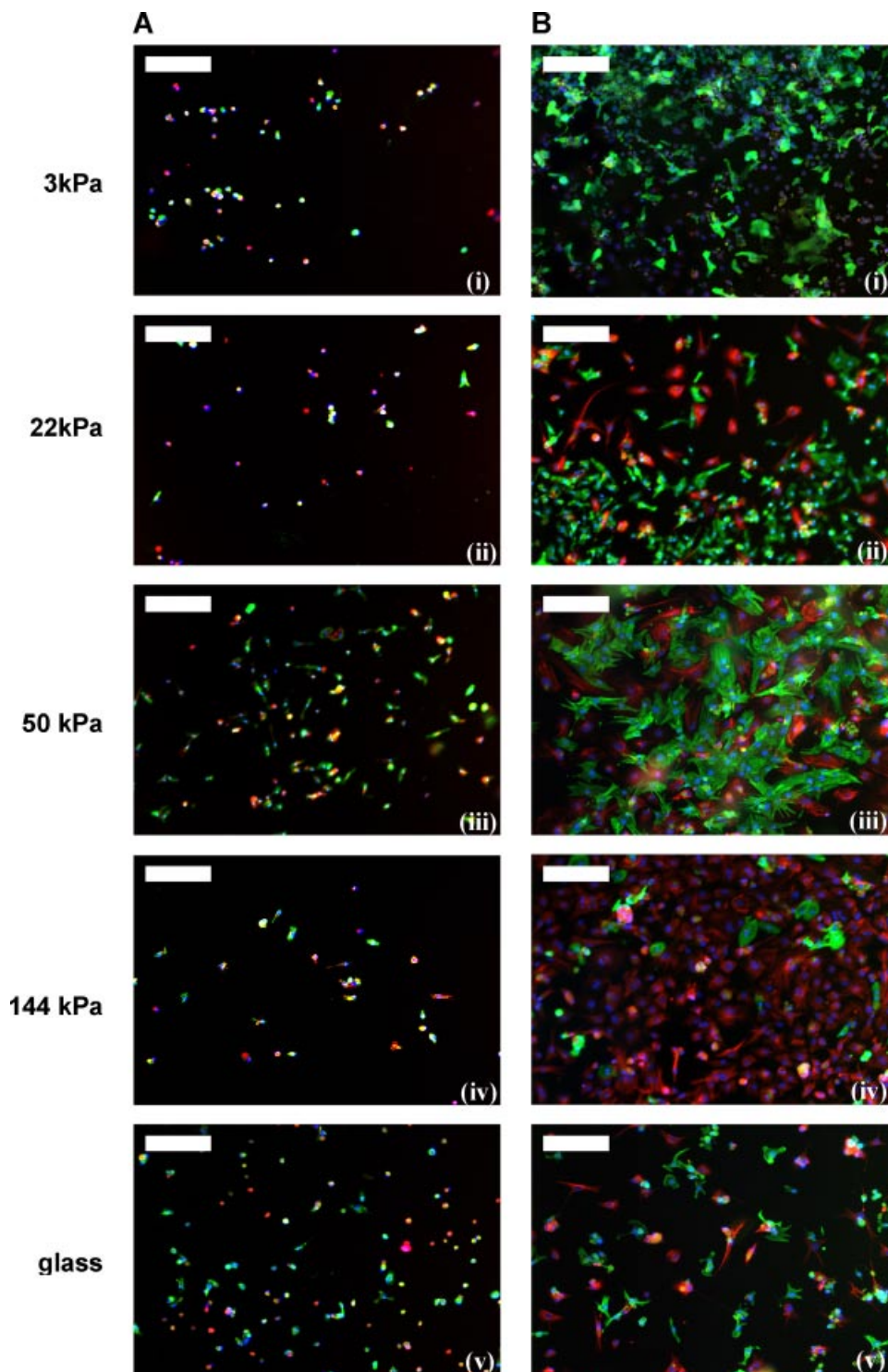


**Figure 5.** Immunostaining for troponin I (green) and vimentin (red) at 12 and 120 h incubation. Cell nuclei stained in DAPI (blue). **A:** 12-h incubation: (i) 3 kPa, (ii) 22 kPa, (iii) 50 kPa, (iv) 144 kPa, (v) glass (infinite stiffness). **B:** 120-h incubation: (i) 3 kPa, (ii) 22 kPa, (iii) 50 kPa, (iv) 144 kPa, (v) glass (infinite stiffness). Images at 10 $\times$  magnification using fluorescence microscopy. Scale bar = 60  $\mu$ m. [Color figure can be seen in the online version of this article, available at [www.interscience.wiley.com](http://www.interscience.wiley.com).]

12 V/cm, to ensure that cells in all substrate groups were contracting. To assess the contraction stress, the hydrogels were analyzed around areas where synchronous and rhythmical beating was observed. Since only CMs are

capable of synchronous and rhythmic contractions, these areas must have contained CM. The poor electrical excitability in the 144 kPa group is likely the result of FB overgrowth and a low percentage of CM in this group

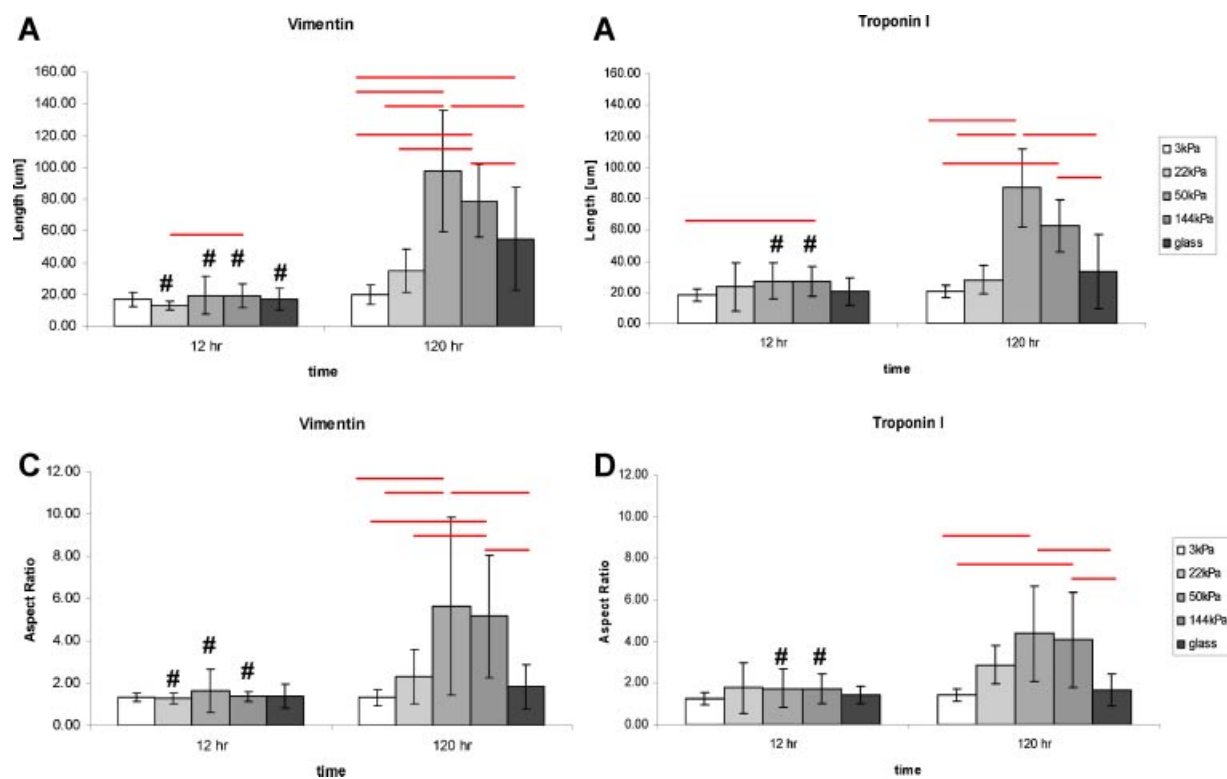


**Figure 6.** Elongation and aspect ratio of heart cells as a function of substrate stiffness measured from phase contrast images. **A, B:** Influence of substrate stiffness on elongation (axial cell length) of (A) fibroblasts (vimentin+) and (B) cardiomyocytes (cardiac troponin I+) as determined from immunostaining. **C, D:** Influence of substrate stiffness on aspect ratio (ratio of axial cell length to radial length) of (C) fibroblasts (vimentin+) and (D) cardiomyocytes (cardiac troponin I+) as determined from immunostaining. Error bars denote standard deviation. Statistical analysis performed using one-way ANOVA,  $P < 0.05$  considered significantly different. #Significantly lower than the same group at 120 h. The measurements were determined from two independent experiments. There were three samples per group, with three pictures per sample taken at  $10\times$ . On average, 20 cells were evaluated at 12 h and 33 cells at the 120 h time point per antibody, per group. [Color figure can be seen in the online version of this article, available at [www.interscience.wiley.com](http://www.interscience.wiley.com).]

(Figs. 5 and 7) at the end of cultivation. Further studies are required, where different percentages of CM and FB will be seeded on the substrates of the identical stiffness to elucidate how contraction force is affected by the cell ratio, independent of the substrate stiffness.

Thus, the only group combining reasonable levels of electrical excitability (Fig. 2) and high contraction force (Fig. 3C) was the 50 kPa gel of stiffness consistent with the native heart. In previous studies, a contraction force between 1 and 2  $\text{mN}/\text{mm}^2$  was reported in the EHT (Zimmermann et al., 2002, 2006), whereas the contraction force for papillary muscle can go up to 56  $\text{mN}/\text{mm}^2$  (Hasenfuss et al., 1991). Thus, the values reported here (e.g.,  $1.60 \pm 0.6 \text{ mN}/\text{mm}^2$  for the 50 kPa substrate, Fig. 3C) are within the physiological range and in agreement with previous findings. The increase in the contraction force in 3–50 kPa substrates (Fig. 3C) is consistent with the increase in cell length and aspect ratio (Fig. 6) as well as the increase in the number of cells exhibiting developed striations (Fig. 8). However, the high contraction force on the 144 kPa substrates is most likely influenced by the presence of a larger number of FB in this group (Fig. 5Biv). It has been demonstrated that stimulation of contraction in ventricular

CM co-cultured with myofibroblasts induces the rise of intracellular  $\text{Ca}^{2+}$  in myofibroblasts (Chilton et al., 2007), which may affect overall force generation.

The greatest degree of heart cell elongation at 50 kPa stiffness (Figs. 5 and 6) increased the opportunity for cell–cell contacts between the CM, which was critical for the development of a synchronous contractions (Boublik et al., 2005). A more compliant substrate (e.g., 3 kPa) may be detrimental to CM elongation, since it would not provide the resistance needed for CM to elongate by lamellipodial protrusions. C2C12 myoblasts grown on substrates from 3 to 400 kPa, exhibited less cell spreading and focal adhesion formation on soft films but formed elongated myotubes with more developed striations on stiffer films (Ren et al., 2008).

Consistent with our observations (Figs. 3B and 5B) others have reported faster cell proliferation on stiffer substrates (Kong et al., 2005; Loftis et al., 2003; Rowley and Mooney, 2002; Wang et al., 2000; Yip et al., 2007). Thus, on the substrate of infinite stiffness such as glass, FB proliferation was enhanced. This led to the higher cell density and as a result, to competition amongst the cells for the substrate attachment sites as well as oxygen and nutrients. Thus, the

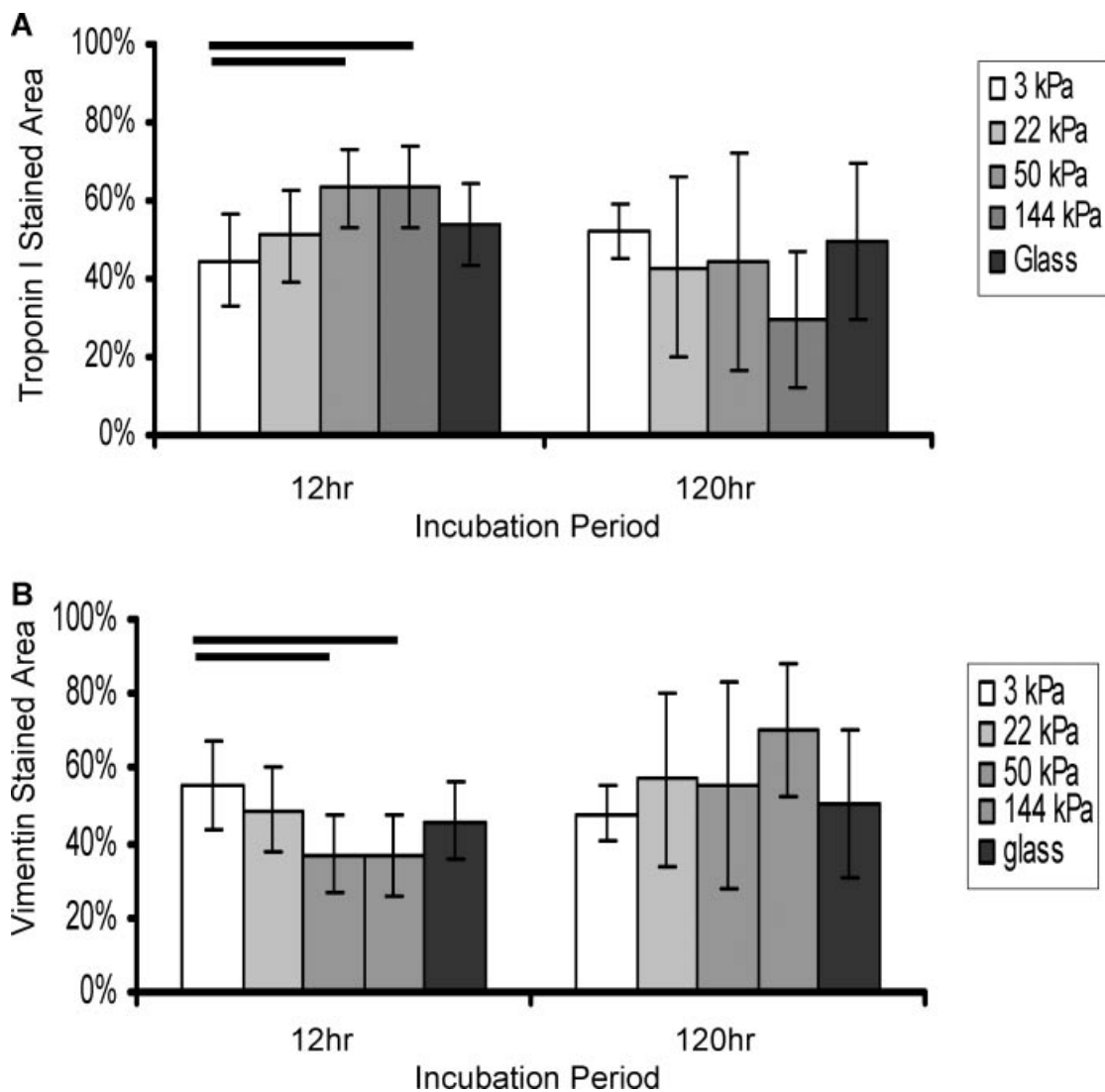


**Figure 7.** Influence of substrate stiffness on cell composition at 12 and 120 h of culture. **A:** Cardiac troponin I identifying cardiomyocytes. **B:** Vimentin identifying non-myocytes, mostly fibroblasts. Expressed as a percentage of the area stained positive relative to the total stained area. Error bars denote standard deviation. Statistical analysis performed using one-way ANOVA,  $P < 0.05$  considered statistically different,  $n = 9$ .

cell viability was decreased on the glass substrate (Fig. 3A). In addition, there may be some stiffness related effects that decreased the cell viability on the glass substrate, since the 144 kPa substrate also exhibited a high cell density at the end of cultivation Figure 3B, with a high FB percentage (Figs. 5Biv and 7B) but it did not exhibit the decrease in cell viability (Fig. 3A).

Taking into account that the composition of the heart cell isolate after one pre-plating step is ~64% CM and ~36% non-myocytes, the latter of which are mostly FB (Brown et al., 2008; Murthy et al., 2006) it is possible to see that the substrates of stiffness 50 and 144 kPa maintained this ratio 12 h after seeding (Fig. 7). At these surfaces, proliferation of FB at later time points (120 h) may have contributed to the increase in their relative percentage. Since after 12 h, there

were 44% CM (Fig. 7A) and 56% FB (Fig. 7B) attached to the 3 kPa surface, we concluded that 3 kPa surfaces likely promoted the initial adhesion of FBs. At the 120 h time point in this group, there were 52% CM (Fig. 7A) and 48% FB (Fig. 7B), with no significant differences to the percentages at 12 h as indicated by statistical analysis. The highest percentage of FB on the infinite stiffness glass substrate (Fig. 5) is consistent with the well-described phenomenon of FB overgrowth in monolayer culture (Boateng et al., 2003; Haddad et al., 1988). In comparison, the 50 kPa substrate had a high fraction of CM at the end of cultivation (Fig. 5). Matrix stiffness may describe the discrepancies observed in heart cell culture on tissue culture plastics versus culture in hydrogels or scaffolds for cardiac tissue engineering. When CM and FB were seeded into hydrogels (Naito et al.,

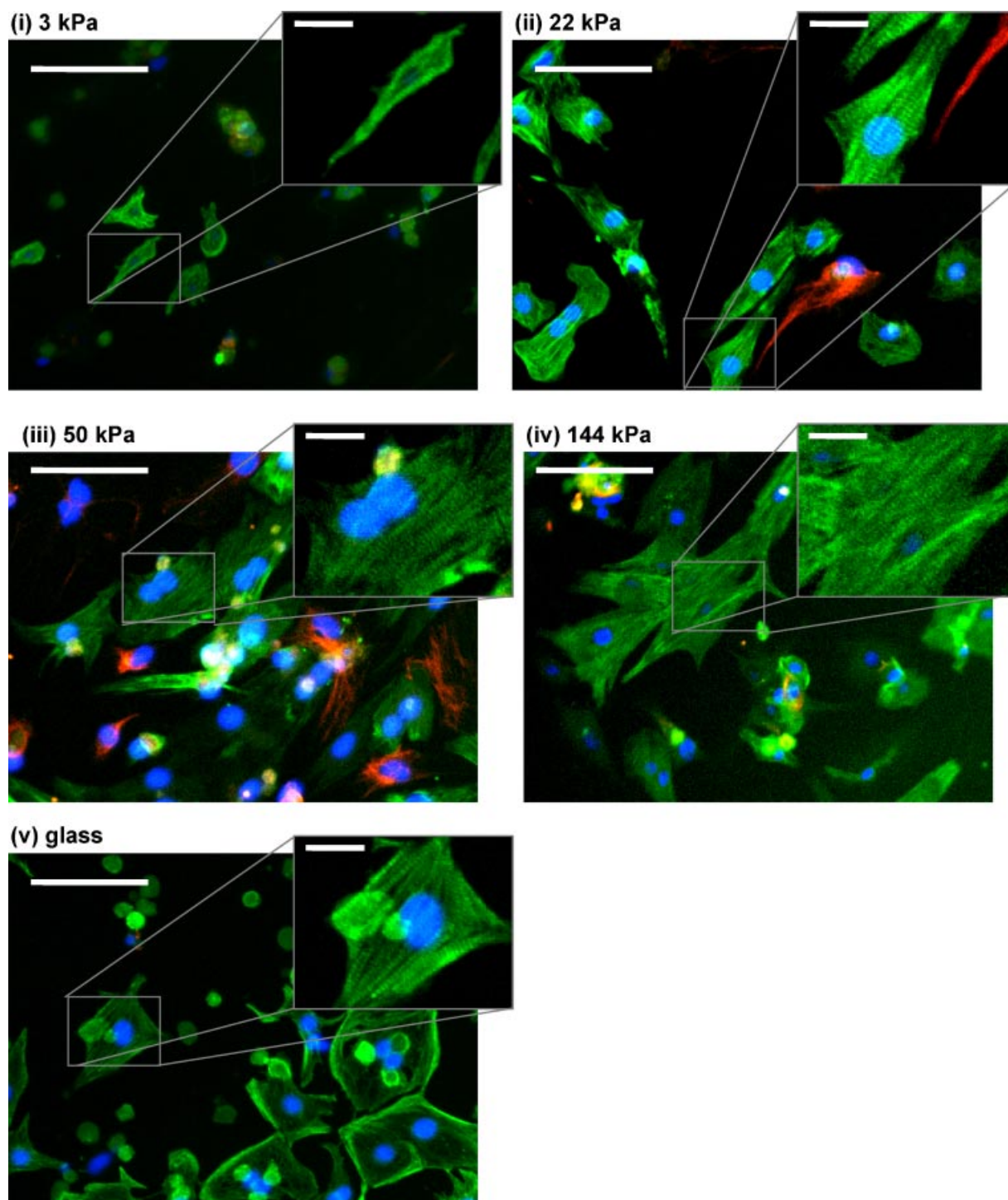


**Figure 8.** Selected images of immunostaining for troponin I (green) and vimentin (red) at 120-h incubation. Cell nuclei stained in DAPI (blue): (i) 3 kPa; (ii) 22 kPa; (iii) 50 kPa, (iv) 144 kPa, and (v) glass (infinite stiffness). All images taken at 10 $\times$  magnification, cropped and enlarged to enhance detail focusing on cardiomyocytes. Scale bars = 30 $\mu$ m. Inset shows sarcomeres at a higher zoom level, scale bar = 30 $\mu$ m. [Color figure can be seen in the online version of this article, available at [www.interscience.wiley.com](http://www.interscience.wiley.com).]

2006) or scaffolds (Radisic et al., 2008b) no FB overgrowth was observed, which may in part be due to the more physiological stiffness of these substrates in comparison to the high stiffness of tissue culture plastics.

As scar tissue contains a high density of cardiac FBs, it is less conducive to contraction (Katwa, 2003; Wu et al., 2006). It was found that CM in cardiac FB-conditioned medium exhibited marked hypertrophy, diminished contractile

capacity, and a distinct phenotype (LaFramboise et al., 2007). Our results indicate that substrates stiffer than 50 kPa, should be avoided for cardiac tissue engineering due to the enhanced FB proliferation and overgrowth (Fig. 7). The poor electrical excitability seen at the highest PA stiffness (144 kPa, Fig. 2) and fewer striations at 144 kPa (Fig. 8) may partially be due to the higher percentage of FB in this group. Due to the enhanced proliferation of FB on stiffer substrates (144 kPa, Fig. 7), the CM may be in direct competition with the FB for adhesion sites. As a result of a reduced number of available adhesion sites, CM elongation may be hampered. The isotropic nature of the PA gels does not direct CM to elongate in a uniform direction. In future studies, micropatterned surfaces of varying stiffness should be explored to facilitate cell–cell junctions in a linear orientation. Further studies are required to elucidate the mechanisms governing stiffness-driven cytoskeletal rearrangement and the effect of substrate stiffness in 3D environment.

## Conclusion

Our results indicate that the stiffness of the extracellular environment affects the phenotype and contractile properties of the heart cells. Overall, taking into account the elongated cell phenotype, maintenance of CM/FB ratio, ability to contract and develop force in response to electrical field stimulation, and the proportion of cells with well-defined sarcomeres and striations, our findings indicate that substrates of stiffness ~50 kPa are the most desirable for cultivation of heart cells. This range is consistent with the stiffness of the native rat heart. The results from this study bring us a step closer to understanding how the mechanical properties of the extracellular environment influence the phenotype of CM and FB under conditions relevant for cardiac tissue engineering. Thus, both the chemical and mechanical properties of the ECM should be considered in the design of scaffolds for cardiac tissue engineering.

This study was supported by Heart and Stroke Foundation of Ontario (HSFO) Grants-in-Aid to M.R. (NA 6077) and C.A.S. (NA6047), National Sciences and Engineering Research Council of Canada Discovery Grants to M.R. (RGPIN 326982-06) and C.A.S. (RGPIN 327627-06), and Ontario Early Researcher Award to C.A.S. and M.R. C.A.S. is supported by Canada Research Chair in Mechanobiology.

## References

- Aoki T, Ohashi T, Matsumoto T, Sato M. 1997. The pipette aspiration applied to the local stiffness measurement of soft tissues. *Ann Biomed Eng* 25:581–587.
- Au HT, Cheng I, Chowdhury MF, Radisic M. 2007. Interactive effects of surface topography and pulsatile electrical field stimulation on orientation and elongation of fibroblasts and cardiomyocytes. *Biomaterials* 28:4277–4293.
- Berry MF, Engler AJ, Woo YJ, Pirolli TJ, Bish LT, Jayasankar V, Morine KJ, Gardner TJ, Discher DE, Sweeney HL. 2006. Mesenchymal stem cell injection after myocardial infarction improves myocardial compliance. *Am J Physiol Heart Circ Physiol* 290:H2196–H2203.
- Boateng SY, Hartman TJ, Ahluwalia N, Vidula H, Desai TA, Russell B. 2003. Inhibition of fibroblast proliferation in cardiac myocyte cultures by surface microtopography. *Am J Physiol Cell Physiol* 285:C171–C182.
- Boublik J, Park H, Radisic M, Tognana E, Chen F, Pei M, Vunjak-Novakovic G, Freed LE. 2005. Mechanical properties and remodeling of hybrid cardiac constructs made from heart cells, fibrin, and biodegradable, elastomeric knitted fabric. *Tissue Eng* 11:1122–1132.
- Brown MA, Iyer RK, Radisic M. 2008. Pulsatile perfusion bioreactor for cardiac tissue engineering. *Biotechnol Prog* 24:907–920.
- Bursac N, Parker KK, Iravanian S, Tung L. 2002. Cardiomyocyte cultures with controlled macroscopic anisotropy: A model for functional electrophysiological studies of cardiac muscle. *Circ Res* 91:e45–e54.
- Caspi O, Lesman A, Basevitch Y, Gepstein A, Arbel G, Habib IH, Gepstein L, Levenberg S. 2007. Tissue engineering of vascularized cardiac muscle from human embryonic stem cells. *Circ Res* 100:263–272.
- Chen WLK, Likhitpanichkul M, Ho A, Simmons CA. (in press). Integration of statistical modeling and high-content microscopy to systematically investigate cell–substrate interactions. *Biomaterials*. Available at <http://dx.doi.org/myaccess.library.utoronto.ca/10.1016/j.biomaterials.2009.12.002>, DOI: 10.1016/j.biomaterials.2009.12.002
- Chilton L, Giles WR, Smith GL. 2007. Evidence of intercellular coupling between co-cultured adult rabbit ventricular myocytes and myofibroblasts. *J Physiol* 583:225–236.
- Chiu LL, Iyer RK, King JP, Radisic M. 2008. Biphasic electrical field stimulation aids in tissue engineering of multicell-type cardiac organoids. *Tissue Eng Part A*. DOI: 10.1089/ten.tea.2007.0244.
- Drury JL, Mooney DJ. 2003. Hydrogels for tissue engineering: Scaffold design variables and applications. *Biomaterials* 24:4337–4351.
- Engelmayr GC, Jr., Cheng M, Bettinger CJ, Borenstein JT, Langer R, Freed LE. 2008. Accordion-like honeycombs for tissue engineering of cardiac anisotropy. *Nat Mater* 7:1003–1010.
- Engler AJ, Griffin MA, Sen S, Bonnemann CG, Sweeney HL, Discher DE. 2004a. Myotubes differentiate optimally on substrates with tissue-like stiffness: Pathological implications for soft or stiff microenvironments. *J Cell Biol* 166:877–887.
- Engler AJ, Richert L, Wong JY, Picart C, Discher DE 2004b. Surface probe measurements of the elasticity of sectioned tissue, thin gels and polyelectrolyte multilayer films: Correlations between substrate stiffness and cell adhesion. *Surf Sci* 570:142–154.
- Engler AJ, Sen S, Sweeney HL, Discher DE. 2006. Matrix elasticity directs stem cell lineage specification. *Cell* 126:677–689.
- Engler AJ, Carag-Krieger C, Johnson CP, Raab M, Tang HY, Speicher DW, Sanger JW, Sanger JM, Discher DE. 2008. Embryonic cardiomyocytes beat best on a matrix with heart-like elasticity: Scar-like rigidity inhibits beating. *J Cell Sci* 121:3794–3802.
- Haddad J, Decker ML, Hsieh LC, Lesch M, Samarel AM, Decker RS. 1988. Attachment and maintenance of adult rabbit cardiac myocytes in primary cell culture. *Am J Physiol Cell Physiol* 255:C19–C27.
- Hasenfuss G, Mulieri LA, Blanchard EM, Holubarsch C, Leavitt BJ, Ittleman F, Alpert NR. 1991. Energetics of isometric force development in control and volume-overload human myocardium. Comparison with animal species. *Circ Res* 68:836–846.
- Iyer RK, Chiu LL, Radisic M. 2009. Microfabricated poly(ethylene glycol) templates enable rapid screening of triculture conditions for cardiac tissue engineering. *J Biomed Mater Res A*. 89:616–631.
- Iyer RK, Chui J, Radisic M. 2009. Spatiotemporal tracking of cells in tissue-engineered cardiac organoids. *J Tissue Eng Regen Med* 3:196–207.
- Jacot JG, McCulloch AD, Omens JH. 2008. Substrate stiffness affects the functional maturation of neonatal rat ventricular myocytes. *Biophys J* 95:3479–3487.
- Katwa LC. 2003. Cardiac myofibroblasts isolated from the site of myocardial infarction express endothelin de novo. *Am J Physiol Heart Circ Physiol* 285:H1132–H1139.
- Kong HJ, Liu J, Riddle K, Matsumoto T, Leach K, Mooney DJ. 2005. Non-viral gene delivery regulated by stiffness of cell adhesion substrates. *Nat Mater* 4:460–464.

- LaFramboise WA, Scalise D, Stoodley P, Graner SR, Guthrie RD, Magovern JA, Becich MJ. 2007. Cardiac fibroblasts influence cardiomyocyte phenotype in vitro. *Am J Physiol Cell Physiol* 292:C1799–C1808.
- Levenberg S, Rouwkema J, Macdonald M, Garfein ES, Kohane DS, Darland DC, Marini R, van Blitterswijk CA, Mulligan RC, D'Amore PA, et al. 2005. Engineering vascularized skeletal muscle tissue. *Nat Biotechnol* 23:879–884.
- Lo CM, Wang HB, Dembo M, Wang YL. 2000. Cell movement is guided by the rigidity of the substrate. *Biophys J* 79:144–152.
- Loftis MJ, Sexton D, Carver W. 2003. Effects of collagen density on cardiac fibroblast behavior and gene expression. *J Cell Physiol* 196:504–511.
- Murthy SK, Sethu P, Vunjak-Novakovic G, Toner M, Radisic M. 2006. Size-based microfluidic enrichment of neonatal rat cardiac cell populations. *Biomed Microdevices* 8:231–237.
- Nag AC. 1980. Study of non-muscle cells of the adult mammalian heart: A fine structural analysis and distribution. *Cytobios* 28:41–61.
- Naito H, Melnychenko I, Didie M, Schneiderbanger K, Schubert P, Rosenkranz S, Eschenhagen T, Zimmermann WH. 2006. Optimizing engineered heart tissue for therapeutic applications as surrogate heart muscle. *Circulation* 114:I72–I78.
- Pelham RJ, Jr., Wang Y. 1997. Cell locomotion and focal adhesions are regulated by substrate flexibility. *Proc Natl Acad Sci USA* 94:13661–13665.
- Peyton SR, Raub CB, Keschrums VP, Putnam AJ. 2006. The use of poly(ethylene glycol) hydrogels to investigate the impact of ECM chemistry and mechanics on smooth muscle cells. *Biomaterials* 27:4881–4893.
- Radisic M, Euloth M, Yang L, Langer R, Freed LE, Vunjak-Novakovic G. 2003. High-density seeding of myocyte cells for cardiac tissue engineering. *Biotechnol Bioeng* 82:403–414.
- Radisic M, Park H, Shing H, Consi T, Schoen FJ, Langer R, Freed LE, Vunjak-Novakovic G. 2004. Functional assembly of engineered myocardium by electrical stimulation of cardiac myocytes cultured on scaffolds. *Proc Natl Acad Sci USA* 101:18129–18134.
- Radisic M, Marsano A, Muidhof R, Wang Y, Vunjak-Novakovic G. 2008a. Cardiac tissue engineering using perfusion bioreactor systems. *Nat Protoc* 3:719–738.
- Radisic M, Park H, Martens TP, Salazar-Lazaro JE, Geng W, Wang Y, Langer R, Freed LE, Vunjak-Novakovic G. 2008b. Pre-treatment of synthetic elastomeric scaffolds by cardiac fibroblasts improves engineered heart tissue. *J Biomed Mater Res A* 86:713–724.
- Ren K, Crouzier T, Roy C, Picart C. 2008. Polyelectrolyte multilayer films of controlled stiffness modulate myoblast cells differentiation. *Adv Funct Mater* 18:1378–1389.
- Rowley JA, Mooney DJ. 2002. Alginate type and RGD density control myoblast phenotype. *J Biomed Mater Res* 60:217–223.
- Semler EJ, Ranucci CS, Moghe PV. 2000. Mechanochemical manipulation of hepatocyte aggregation can selectively induce or repress liver-specific function. *Biotechnol Bioeng* 69:359–369.
- Shapira-Schweitzer K, Seliktar D. 2007. Matrix stiffness affects spontaneous contraction of cardiomyocytes cultured within a PEGylated fibrinogen biomaterial. *Acta Biomater* 3:33–41.
- Subramanian A, Lin HY. 2005. Crosslinked chitosan: Its physical properties and the effects of matrix stiffness on chondrocyte cell morphology and proliferation. *J Biomed Mater Res A* 75:742–753.
- Tandon N, Cannizzaro C, Chao PH, Muidhof R, Marsano A, Au HT, Radisic M, Vunjak-Novakovic G. 2009. Electrical stimulation systems for cardiac tissue engineering. *Nat Protoc* 4:155–173.
- Theret DP, Levesque MJ, Sato M, Nerem RM, Wheeler LT. 1988. The application of a homogeneous half-space model in the analysis of endothelial cell micropipette measurements. *J Biomech Eng* 110:190–199.
- Wang HB, Dembo M, Wang YL. 2000. Substrate flexibility regulates growth and apoptosis of normal but not transformed cells. *Am J Physiol Cell Physiol* 279:C1345–C1350.
- Wu RX, Laser M, Han H, Varadarajulu J, Schuh K, Hallhuber M, Hu K, Ertl G, Hauck CR, Ritter O. 2006. Fibroblast migration after myocardial infarction is regulated by transient SPARC expression. *J Mol Med* 84:241–252.
- Yang Z, Lin JS, Chen J, Wang JH. 2006. Determining substrate displacement and cell traction fields—A new approach. *J Theor Biol* 242:607–616.
- Yeung T, Georges PC, Flanagan LA, Marg B, Ortiz M, Funaki M, Zahir N, Ming W, Weaver V, Janmey PA. 2005. Effects of substrate stiffness on cell morphology, cytoskeletal structure, and adhesion. *Cell Motil Cytoskeleton* 60:24–34.
- Yip CYY, Chen J-H, Simmons CA. 2008. Technologies and Applications for Engineering Substrate Mechanics to Regulate Cell Response. In: Khademhosseini A, Borenstein J, Toner M, Takayama S, editors. *Micro and nanoengineering of the cell microenvironment: Technologies and applications*. Boston: Artech House. pp. 161–183.
- Zimmermann WH, Schneiderbanger K, Schubert P, Didie M, Munzel F, Heubach JF, Kostin S, Nehuber WL, Eschenhagen T. 2002. Tissue engineering of a differentiated cardiac muscle construct. *Circ Res* 90:223–230.
- Zimmermann WH, Melnychenko I, Wasmeier G, Didie M, Naito H, Nixdorff U, Hess A, Budinsky L, Brune K, Michaelis B, et al. 2006. Engineered heart tissue grafts improve systolic and diastolic function in infarcted rat hearts. *Nat Med* 12:452–458.